Extreme Midinfrared Nonlinear Optics in Semiconductors

Alan H. Chin,[1,*] Oscar G. Calderón,[1,†] and Junichiro Kono[2]

[1]*W. W. Hansen Experimental Physics Laboratory, Stanford University, Stanford, California 94305*
[2]*Department of Electrical and Computer Engineering, Rice University, Houston, Texas 77005*

(Received 29 August 2000)

We have observed extreme nonlinear optical phenomena produced by intense midinfrared (MIR) pulses in semiconductors. These phenomena include multiple off-resonance optical sidebands (up to ± 3 MIR photons interacting with a near-infrared photon), multiple MIR harmonics (up to the seventh harmonic), and significant broadening and modification of MIR harmonic spectra. The generation of these extreme MIR nonlinear optical phenomena is primarily aided by cross-phase modulation.

DOI: 10.1103/PhysRevLett.86.3292 PACS numbers: 42.65.Ky, 42.50.Hz

The desire for broad-bandwidth communications systems has led to increasing interest in the development of terahertz (THz) electronics [1], i.e., the area between electronics and photonics where currently a technology gap exists. Because nonlinear optical phenomena (especially with strong fields) will likely play a role in future THz devices [2,3], midinfrared (MIR) and far-infrared (FIR) nonlinear optics may serve as a basis for future device development. While many interesting nonlinear optical phenomena, such as high-order harmonic generation [4] and continuum generation [5–7], have been extensively studied using ultrafast laser sources in the visible or near-infrared (NIR), relatively few studies of nonlinear optical phenomena have been made using intense light in the MIR [2,8,9] or FIR [10,11]. Here, we examine sideband generation (i.e., nondegenerate sum-frequency and difference-frequency generation) and harmonic generation using intense MIR pulses in semiconductors under conditions where extreme behavior is observed due to the strong fields at long (compared to visible) wavelengths used. Under these conditions, we observed the generation of sidebands involving the interaction of up to three MIR photons with a NIR photon and the generation of MIR harmonics up to the seventh harmonic. In some cases, we observed significant broadening and modulation in the spectrum of MIR harmonics. The appearance of these extreme nonlinear optical phenomena is primarily aided by cross-phase modulation (XPM) [12–14], i.e., the influence of self-phase modulation (SPM) in one beam on other beams in nonlinear wave mixing processes. The generation of these phenomena is also aided by the low dispersion in many semiconductors in the MIR range.

The source of intense pulses used for these extreme MIR nonlinear optics studies is an optical parametric amplifier pumped by a Ti:sapphire based regenerative amplifier. The system produces pulses at a 1 kHz repetition rate with either $\sim$1 ps or $\sim$200 fs pulse duration, and (with difference-frequency mixing of the signal and idler) wavelengths from 3 to 10 μm. For these studies, we used pulses at wavelengths of 3.5 or 6.2 μm (where atmospheric absorption is negligible). We used two methods to study extreme MIR nonlinear optics in semiconductors. In the first method, we measured the NIR spectrum after nonlinear wave mixing of intense NIR and MIR pulses in a semiconductor. Temporal overlap was achieved by varying the optical path of the MIR beam with respect to the NIR beam. In the second method, we measured the spectrum of intense MIR pulses after transmission through a semiconductor.

Using the first method, we observed multiple off-resonance optical sideband generation in semiconductors. As shown in Fig. 1, the 800 nm (1.55 eV) NIR probe pulse spectrum is significantly modified in the presence of intense MIR fields to possess multiple sidebands that are spaced by the MIR photon energy. The data in Fig. 1(a) were obtained in polycrystalline ZnSe (3 mm thick) using $\sim$1 ps pulses of either 3.5 μm wavelength (0.35 eV) with peak intensity of $\sim 2 \times 10^{10}$ W/cm^2 or 6.2 μm wavelength (0.22 eV) with peak intensity of $\sim 3 \times 10^9$ W/cm^2. We observed sum-frequency and difference-frequency mixing (± 1 MIR photon sidebands) as well as higher-order wave mixing, with up to ± 3 MIR photon sidebands (with 6.2 μm MIR pulses) observed in the spectral range of the detectors (Si and InGaAs photodiodes) used. Previous studies of sideband generation in semiconductors relied on *resonant* enhancement of the nonlinear optical susceptibility [10]. Here, we observed multiple *nonresonant* sidebands in semiconductors. The ± 1 (± 2) MIR photon sidebands are linearly (quadratically) dependent on the MIR intensity up to the maximum MIR intensity used with the $\sim$1 ps pulses. All of the sidebands are linearly dependent on the NIR intensity. We also observed multiple optical sidebands in ZnS and ZnTe, demonstrating the lack of system specificity due to the nonresonant nature of the wave mixing. Using higher intensities with shorter pulses, we observed interesting spectral structure and broadening in the bandwidth (in excess of the transform limited bandwidth) of the sidebands. This behavior is shown in Fig. 1(b), where we see the ± 1 MIR sidebands in ZnTe(100) using $\sim$200 fs pulses of wavelength $\sim$3.5 μm with intensities up to $\sim 10^{11}$ W/cm^2. These data show an increase in both the broadening and the structure of the sideband spectra with increasing intensity. With varying temporal overlap

 0031-9007/01/86(15)/3292(4)$15.00

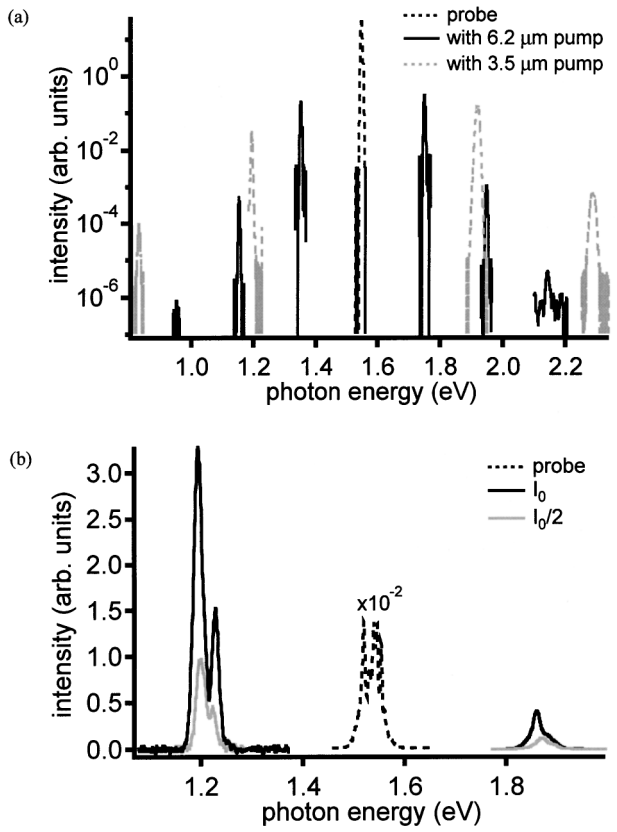

FIG. 1. (a) Optical sidebands in polycrystalline ZnSe (3 mm thick) generated when a MIR pump pulse and a 800 nm (1.55 eV) probe pulse (dashed line) are overlapped (both pulses are ~1 ps). The sidebands generated by 3.5 μm (0.35 eV) at $\sim 2 \times 10^{10}$ W/cm^2 (gray dashed line) and 6.2 μm (0.22 eV) at $\sim 3 \times 10^9$ W/cm^2 (black line) MIR pump are shown. (b) ± 1 MIR sidebands in 150 μm thick ZnTe(100) when a 800 nm (1.55 eV) probe pulse (dashed line) is overlapped with a ~3.5 μm (0.35 eV) MIR pulse (both pulses are ~200 fs) with intensities of $I_0 \sim 10^{11}$ W/cm^2 (black line) and $I_0/2$ (gray line).

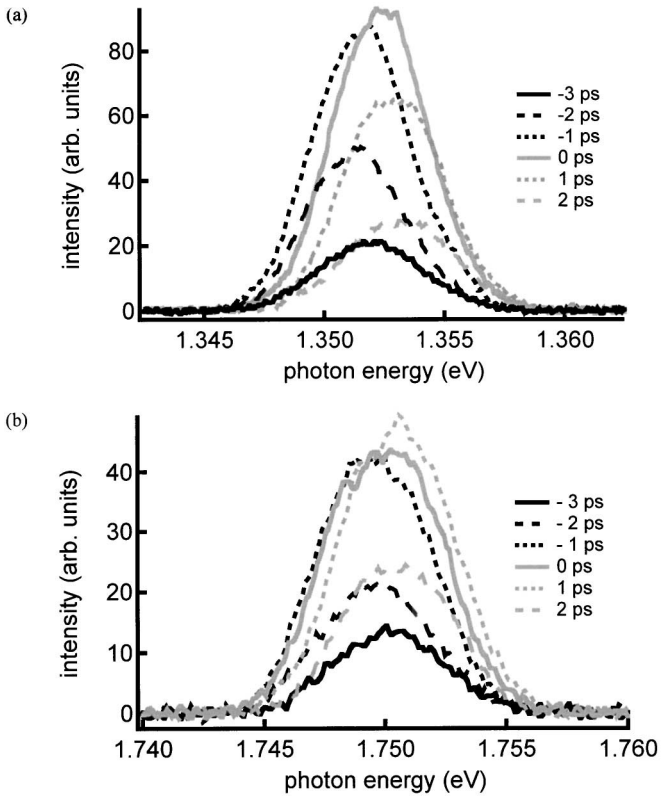

FIG. 2. (a) -1 sideband spectra and (b) $+1$ sideband spectra in polycrystalline ZnSe (3 mm thick) for different time delays (negative time delay corresponds to MIR pulses arriving before NIR pulses) between 6.2 μm (0.22 eV) MIR pulses at $\sim 3 \times 10^9$ W/cm^2 and 800 nm (1.55 eV) NIR pulses (both pulses are ~1 ps).

between the MIR and NIR pulses, we also observed spectral shifts. Figure 2 shows the sideband spectra as a function of time delay between 6.2 μm MIR and 800 nm NIR pulses for the ~1 ps in polycrystalline ZnSe (3 mm thick) for the ± 1 MIR sidebands. The sideband spectra change in both intensity and peak location as the NIR pulse interacts with different temporal sections of the MIR pulse.

Using the second method, we observed multiple MIR harmonics below the band edge in semiconductors. Figure 3(a) shows the multiple harmonics observed in polycrystalline ZnS (2 mm thick) using ~1 ps pulses at 3.5 μm, with a peak intensity of $\sim 2 \times 10^{10}$ W/cm^2. Up to the maximum MIR intensity used with the ~1 ps pulses, the second, third, and fourth harmonics are measured to have quadratic, cubic, and quartic dependence with the MIR intensity, respectively. While third and higher harmonics have been observed from solid surface [15], and MIR harmonics have been observed in gases [8] and liquids [9], we observed multiple (up to fifth harmonic) MIR harmonics in *bulk* semiconductors. With higher MIR intensity ($\sim 10^{11}$ W/cm^2) using shorter (~200 fs) pulses at ~3.9 μm, we also observed an interesting broadening of the spectrum (in excess of the transform limited bandwidth) of MIR harmonics. An extreme case of this broadening is shown in Fig. 3(b), where multiple (up to seventh) MIR harmonics are seen to exhibit both spectral broadeing and overlap between the harmonics to form what we refer to as a harmonic continuum. Individual harmonics are also observed to exhibit unusual spectral modulation under certain conditions. Shown in Fig. 4(a) is the third harmonic in a GaAs(100) crystal (350 μm thick). In this case, the broadened spectrum contains structure that is reminiscent of spectral structure due to SPM [16], but the broadening is present in a *harmonic* instead of the fundamental.

We believe that several factors contribute to the generation of the observed extreme MIR nonlinear optical phenomena by minimizing phase mismatch between the relevant beams. Two such factors are the low dispersion that exists at wavelengths in between phonon absorption and interband absorption in semiconductors and the long (compared to visible) wavelengths used. Low dispersion allows a longer interaction length (i.e., length over which maximum harmonic intensity is produced [17], also

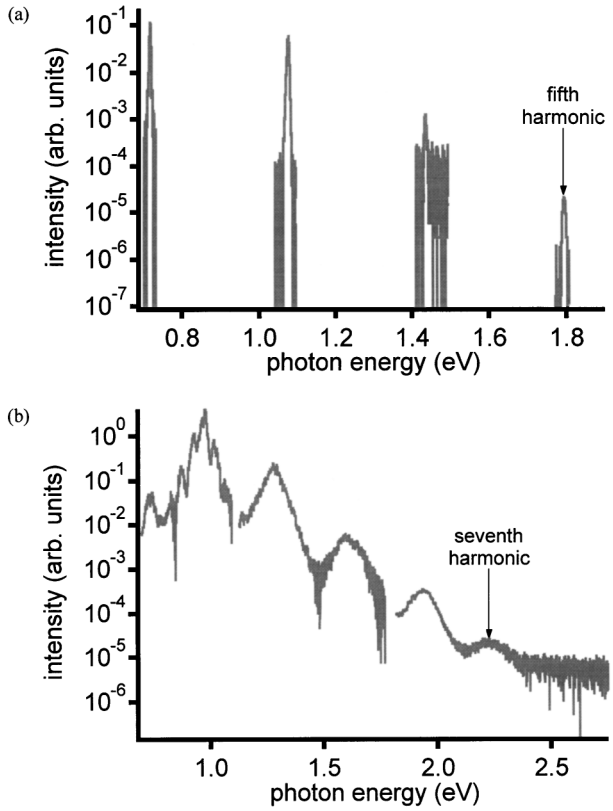

FIG. 3. (a) MIR harmonics in polycrystalline ZnS (2 mm thick) using 3.5 μm (0.35 eV), $\sim$1 ps, $\sim 2 \times 10^{10}$ W/cm^2 MIR pulses. (b) MIR harmonics in polycrystalline ZnSe (3 mm thick) using $\sim$3.9 μm (0.32 eV), $\sim$200 fs, $\sim 10^{11}$ W/cm^2 MIR pulses.

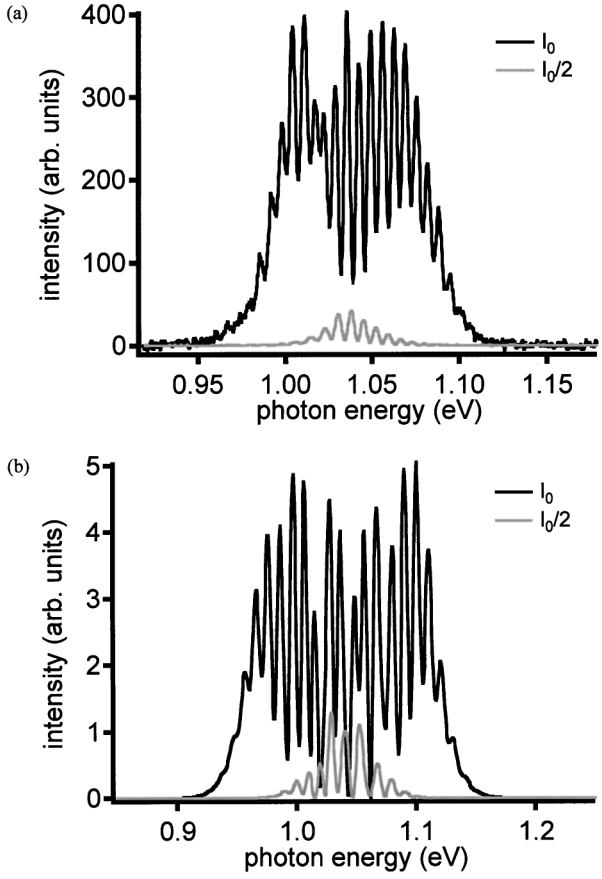

FIG. 4. (a) Spectral broadening and modulation in the third harmonic of 3.5 μm (0.35 eV), $\sim$200 fs MIR in 350 μm thick GaAs(100), using $I_0 \sim 10^{11}$ W/cm^2 (black line) and $I_0/2$ (gray line). (b) Simulation of the spectral broadening and modulation in the third harmonic, assuming pulse splitting and SPM occurs.

known as coherence length) for sideband/harmonic generation. To illustrate this point, consider the case of second harmonic generation in GaAs in regions of low and high dispersion. To generate the second harmonic using a fundamental wavelength of 6 μm (low dispersion), the interaction length is $\sim$75 μm, whereas, to generate second harmonic using a fundamental wavelength of 1.6 μm (high dispersion), the interaction length is $\sim$1 μm. Longer wavelengths intrinsically yield longer interaction lengths due to the slower phase variation. Consequently, the generation of sidebands/harmonics is more efficient at longer wavelengths, as is demonstrated by the sideband data in Fig. 1(a). In spite of these factors, the estimated interaction lengths (up to $\sim$100 μm) are still much shorter than the sample thicknesses used here ($\sim$1 mm). Thus, without any spectral modifications, significant phase mismatch exists in the samples considered here.

One factor that can alleviate the remaining phase mismatch is the influence of SPM on sideband/harmonic generation, which is known as XPM [12,18]. Under the excitation conditions used in the experiment, significant phase shifts due to SPM are expected to occur in the MIR beam. For example, using $\sim 2 \times 10^{10}$ W/cm^2 at a wavelength of 3.5 μm passing through 350 μm of GaAs (nonlinear refractive index, $n_2 \sim 3 \times 10^{-10}$ esu [19]), the estimated intensity-induced phase shift is $\sim$1 rad. Self-phase modulation generates additional bandwidth in the fundamental, which alleviates any strong thickness dependence of phase matching through XPM by providing a distribution of wave vectors that contributes to the generation of each sideband/harmonic wavelength. This consequence of XPM, in combination with the low dispersion and long wavelength light used, allows multiple sideband/harmonic generation to be more easily observable using MIR rather than visible fundamental frequencies. To verify this, we performed numerical calculations that take into account $\chi^{(3)}$ processes involving SPM of the MIR, $\chi^{(N)}$ processes for the sideband/harmonic generation process under the influence of XPM, and the appropriate phase matching [20]. We obtained good agreement between the calculations and the data.

In addition to alleviating phase mismatch, XPM may be the cause of the observed spectral modification in the sidebands and harmonics [12,18,21]. The observed spectral shifting of the sidebands with time delay between the MIR and NIR pulses (Fig. 2) may be explained by the MIR pulse inducing different amounts of phase change seen by the NIR pulse with different temporal overlap. With $n_2 > 0$, as the NIR pulse interacts with the rising (falling) edge of the MIR pulse, the NIR spectrum is redshifted

(blueshifted) (this is sometimes called induced-phase modulation [14,21]). The spectral shift of the NIR spectrum leads to the spectral shift of the sidebands with time delay between the MIR and NIR pulses observed in Fig. 2. Along with the spectral shifts, XPM may also be the cause of the observed spectral broadening [12,18] in the sidebands [Fig. 1(b)] and harmonics [Figs. 3(b) and 4(a)]. The overall spectral width in an individual sideband/harmonic is modified by spectral broadening of the fundamental MIR beam being mapped onto the sideband/harmonic during propagation. Because XPM also aids in alleviating any phase mismatch (as described above), XPM may also contribute to the larger than expected increase in the integrated intensity of the sideband/harmonic with increasing fundamental intensity observed in Figs. 1(b) and 4(a). The slow period spectral modulation may be attributed to the amplitude modulation caused by SPM in the MIR that is mapped onto the sideband/harmonic.

While some of the spectral modulation can be explained by XPM, it cannot explain the formation of periodic (in frequency) spectral modulation. We attribute the periodic spectral modulation that is observed in the third harmonic in GaAs [Fig. 4(a)] to pulse splitting in the fundamental [5], which translates into pulse splitting in the harmonic. Since we expect significant self-focusing and SPM to occur in this case, it is reasonable to assume that pulse splitting of the fundamental also occurs [5,7]. Interference between the time separated harmonic pulses produces the periodic spectral modulation [22]. To verify this, numerical calculations described above were performed for the higher intensity and shorter MIR pulse conditions, assuming the fundamental MIR pulse consists of two temporally separated pulses [20]. Assuming fundamental pulses ($\sim$200 fs) separated by $\sim$400 fs with one pulse $\sim$1.5 times larger than the other, but with the overall energy in the pulse preserved, the simulation qualitatively agrees with the data, as shown in Fig. 4(b).

In conclusion, we have observed extreme MIR nonlinear optical phenomena in semiconductors. We observed multiple sidebands and multiple harmonics below the band edge of semiconductors in an intensity regime where SPM is expected. We also observed significant spectral broadening in harmonics using MIR pulses where significant SPM and pulse splitting of the fundamental is expected. With high enough intensity, the spectral broadening may be such that spectral overlap between harmonics occurs, forming a harmonic continuum. These extreme MIR nonlinear optical phenomena are primarily the result of XPM, i.e., SPM of the fundamental providing additional bandwidth that alleviates any phase mismatch and increases the bandwidth of the sidebands or harmonics generated. These phenomena are also aided by the low dispersion that occurs in semiconductors in the wavelength range between phonon resonances and the interband absorption edge. In addition, we observed both broadening and modulation in the third harmonic spectrum in GaAs, which may indicate that pulse splitting in the harmonic (due to pulse splitting in the MIR fundamental) in addition to SPM is occurring under these conditions. The observed extreme MIR nonlinear optical phenomena may play a role in future THz electronics (e.g., for frequency conversion).

We gratefully acknowledge support from NSF Grant No. DMR-0049024, ONR N00014-94-1-1024, the Japan Science and Technology Corporation PRESTO Program, and the NEDO International Joint Research Grant Program. O. G. C. is supported by Becas Computense "del Amo." We thank Dr. T. Kimura, A. P. Mitchell, and J. Guo for their assistance with the experiments, and Professor H. A. Schwettman and Professor T. I. Smith for their support. A. H. C. thanks Dr. C. V. Bennett for enlightening discussions.

*Present address: Lawrence Livermore National Laboratory, P.O. Box 808, Livermore, California 94551.
†Permanent address: Departamento Optica, Universidad Complutense de Madrid, Ciudad Universitaria s/n, 28040 Madrid, Spain.

[1] J. M. Chamberlain and R. E. Miles, *New Directions in Terahertz Technology* (Kluwer, Dordrecht, 1997).
[2] A. H. Chin, J. M. Bakker, and J. Kono, Phys. Rev. Lett. **85**, 3293 (2000).
[3] K. Johnsen and A.-P. Jauho, Phys. Rev. B **57**, 8860 (1998).
[4] A. Rundquist *et al.,* Science **280**, 1412 (1998).
[5] A. A. Zozulya *et al.,* Phys. Rev. Lett. **82**, 1430 (1999); J. K. Ranka, R. W. Schirmer, and A. L. Gaeta, Phys. Rev. Lett. **77**, 3783 (1996).
[6] A. Brodeur and S. L. Chin, Phys. Rev. Lett. **80**, 4406 (1998).
[7] D. Strickland and P. B. Corkum, J. Opt. Soc. Am. B **11**, 492 (1994).
[8] B. Sheehy *et al.,* Phys. Rev. Lett. **83**, 5270 (1999).
[9] R. Zürl and H. Graener, Appl. Phys. B **66**, 213 (1998).
[10] J. Kono *et al.,* Phys. Rev. Lett. **79**, 1758 (1997); C. Phillips *et al.,* Appl. Phys. Lett. **75**, 2728 (1999); W. L. Faust and C. H. Henry, Phys. Rev. Lett. **17**, 1265 (1966).
[11] A. Mayer and F. Keilmann, Phys. Rev. B **33**, 6954 (1986); **33**, 6962 (1986).
[12] A. M. Zheltikov, N. I. Koroteev, and A. N. Naumov, JETP **88**, 857 (1999).
[13] Y. B. Band, C. Radzewicz, and J. S. Krasinski, Phys. Rev. A **49**, 517 (1994).
[14] R. R. Alfano and P. P. Ho, IEEE J. Quantum Electron. **24**, 351 (1988).
[15] Y.-S. Lee, M. H. Anderson, and M. C. Downer, Opt. Lett. **22**, 973 (1997); T. Tsang, Phys. Rev. A **54**, 5454 (1996).
[16] R. H. Stolen and C. Lin, Phys. Rev. A **17**, 1448 (1978).
[17] G. R. Fowles, *Introduction to Modern Optics* (Dover, Mineola, New York, 1989).
[18] P. P. Ho *et al.,* Appl. Phys. Lett. **54**, 111 (1989); H. J. Bakker *et al.,* Phys. Rev. A **42**, 4085 (1990).
[19] A. A. Said *et al.,* J. Opt. Soc. Am. B **9**, 405 (1992).
[20] O. G. Calderón, A. H. Chin, and J. Kono, Phys. Rev. A (to be published).
[21] G. P. Agrawal, P. L. Baldeck, and R. R. Alfano, Phys. Rev. A **40**, 5063 (1989).
[22] R. M. Rassoul *et al.,* Opt. Lett. **22**, 268 (1997).